Article

Fiber Reinforced Concrete with Natural Plant Fibers—Investigations on the Application of Bamboo Fibers in Ultra-High Performance Concrete

Can Mark Bittner * and Vincent Oettel

Institute of Concrete Construction, Leibniz University Hannover, 30167 Hanover, Germany
* Correspondence: bittner@ifma.uni-hannover.de

Abstract: Natural plant fibers represent a sustainable alternative to conventional fiber reinforcement materials in cementitious materials due to their suitable mechanical properties, cost-effective availability and principle carbon neutrality. Due to its high tensile strength and stiffness as well as its worldwide distribution along with rapid growth, bamboo offers itself in particular as a plant fiber source. In experimental studies on concrete beams reinforced with plant fibers, a positive influence of the fibers on the flexural behavior was observed. However, the load-bearing effect of the fibers was limited by the poor bond, which can be attributed, among other things, to the swelling behavior of the fibers. In addition, the plant fibers degrade in the alkaline environment of many cementitious building materials. In order to improve the bond and to limit the alkalinity and to increase the durability, the use of ultra-high performance concrete (UHPC) offers itself. Since no tests have been carried out, investigations on the flexural behavior of UHPC with bamboo fibers were carried out at the Institute of Concrete Construction of Leibniz University Hannover. The test results show a significantly improved load-bearing behavior of the fibers and the enormous potential of the combination of UHPC and bamboo fibers.

Keywords: bamboo fibers; ultra-high performance concrete; plant fiber-reinforced concrete; four-point bending test; post-crack behavior; performance

1. Introduction

Cementitious building materials such as concrete and mortar have become indispensable in modern construction due to their availability, cost-effective production, free formability, durability and compressive strengths of more than 200 N/mm² [1]. In addition to their advantages, however, concretes also have some structural disadvantages. For example, the tensile strength is often less than 1/10 to 1/20 of the compressive strength. Moreover, with their brittle failure, concretes exhibit unfavorable fracture behavior. To compensate the low tensile strength and achieve a higher load-bearing capacity, ductility and toughness, concretes are usually used in combination with building materials with a high tensile strength, which can absorb tensile stresses and bridge cracks.

In addition to the reinforced concrete construction method, in which concrete components are reinforced by steel reinforcement bars, fiber concretes are also increasingly being used. In this case, fibers are added to the concrete during the production process, which prevent or delay the development of microcracks in the hardened state and improve the post-crack behavior of the cracked concrete [2–6]. Due to the high tensile strength and stiffness as well as the corrosion protection provided by the alkaline environment of the concrete, fibers made of steel have been predominantly used for this purpose. However, other man-made fibers made of glass, carbon or polymers are also used in the construction industry [3,7,8]. Yet, man-made fibers have some disadvantages. For example, their production is energy intensive, releases comparatively high amounts of greenhouse gases, and is associated with high consumption of non-renewable resources [9,10]. In addition, their

availability is limited in many regions of the world. For instance, of the 54 African countries, only two are able to produce steel in significant quantities for their own economies [11,12]. The remaining African nations, as well as many nations in Southeast Asia and South America, rely on imported steel with highly volatile prices and have to compete for this important construction material on the world market [12,13]. The other man-made fibers made of glass, carbon or polymers are often not a real alternative, as they are even more limited in availability and usually their cost exceeds that of steel [14,15]. Accordingly, there is a need, especially in these regions of the world, for local reinforcement alternatives that are as cost-effective and environmentally friendly as possible to enable the construction and expansion of a safe and sustainable modern building structure.

Plant fibers offer a natural alternative to man-made fibers. Although the use of plant fibers in polymer materials has already become established [16,17], plant fibers have so far only very rarely been used in concretes. Although some investigations have been carried out regarding the mechanical properties of plant fiber reinforced concretes and mortars, the results of the investigations were often insufficient for practical implementation (e.g., [7,18,19]). In addition, normal-strength concretes reinforced with plant fibers exhibit some problems that have not yet been solved, such as insufficient bonding between fibers and concrete and insufficient durability. The use of ultra-high performance concrete (UHPC) represents a promising approach to solving these problems. For this purpose, experimental investigations on bamboo fiber-reinforced UHPC have been carried out at the Institute of Concrete Construction (IfMa) of Leibniz University Hannover, which will be reported on in the following. This is preceded by an analysis of possible plant fiber types for use in concrete and a compilation and analysis of the investigations already carried out on with plant fibers reinforced normal-strength concretes.

2. State of Research

2.1. Plant Fibers

Plant fibers are natural composite materials with a polylaminar cell structure. The individual cell walls are composed of different proportions of hemicellulose, lignins and cellulose [20–22]. The cellulose molecules which are arranged in chains form the basis of the fibers and largely determine the tensile properties of the plant fibers [23]. Besides the cellulose content, the angle of inclination of the cellulose chains to the longitudinal fiber axis, the microfibril angle (MFA), is also relevant. The tensile strength and stiffness of the fibers decrease with increasing MFA, whereas the elongation at break increases with increasing MFA [21,23,24].

Depending on the plant species, the individual fibers usually have a length of a few millimeters to a few centimeters and are grouped in fiber bundles, which can comprise less than 10 to well over 100 fibers [20]. Despite the higher tensile strength of single fibers [21,23], fiber bundles are predominantly used in concretes and mortars. Reasons for this are the difficult mechanical separation of the single fibers, their small diameter of only about 20 µm and the low bending stiffness [20,21,23]. Due to the different composition, geometry and structure of the fiber (-bundles), the plant fibers also exhibit deviating mechanical properties. Table 1 provides an overview of the typical properties of selected natural plant fiber bundles. It can be seen that coir has a very low tensile strength, whereas Sisal and Bamboo have a tensile strength similar to reinforcement steel and Flax and Hemp have a tensile strength comparable to high strength steel.

With regard to a globally sustainable application of plant fibers in concretes, many other factors are relevant in addition to the mechanical properties. Besides the use of pesticides, fungicides and fertilizers during cultivation, local availability—especially in the so-called developing countries—is also important. Hemp and flax fibers have very good mechanical properties, but their cultivation area is limited to the temperate climate zone, which is suboptimal for global application [20]. So-called developing countries are mainly found in tropical and subtropical climatic regions, where coconut palms and bamboo (Figure 1) are the most widely grown natural fiber plants [20,25–27]. The cultivation

of coconut palms in coastal regions is associated with lower freshwater requirements due to their high saltwater tolerance [20,28], but the coir obtained from coconuts has comparatively low mechanical properties in comparison to the other plant fibers (Table 1). Bamboo offers many advantages as a plant fiber source due to its early harvest maturity after 3 to 5 years [29,30], simple harvesting and processing, vegetative reproduction via rhizomes [31], protection of the soil from erosion [32], and positive influence on the water table [12]. Combined with high tensile strength and high stiffness, bamboo fibers therefore offer themselves as a natural reinforcement material in concretes.
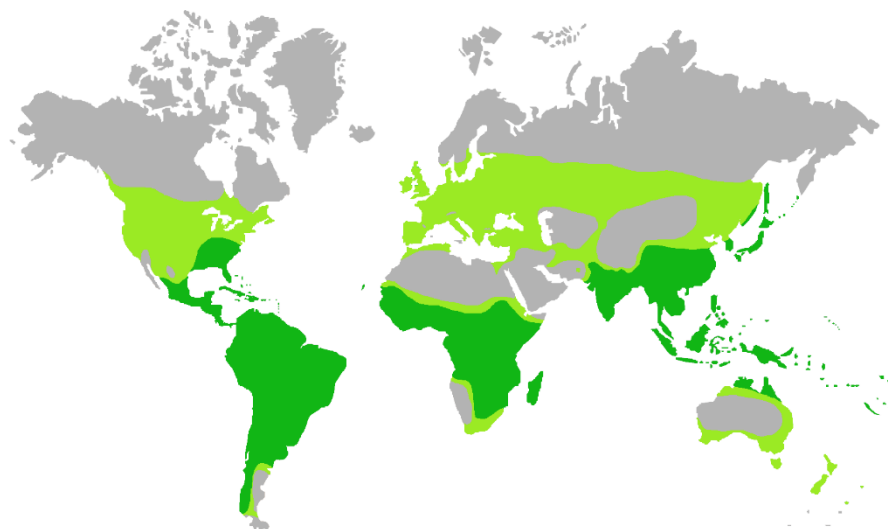

Figure 1. Native regions (dark green) and (possible) cultivation areas (light green) of bamboo according to [25,27,31,39,40].

Table 1. Typical properties of various selected plant fiber bundles [20,33–38].

Fiber	Cellulose [%]	Relevant MFA [°]	Tensile Strength [N/mm^2]	Module of Elasticity [N/mm^2]
Flax	70	7	1000	60,000
Hemp	65	4	700	50,000
Sisal	65	17	450	40,000
Coir	35	45	150	5000
Bamboo	60	8	400	35,000

2.2. Plant Fiber Reinforced Cement Based Composites

The flexural strength and toughness of plant fiber reinforced concretes (PFRC) have already been investigated in several studies. Ali et al. [41] investigated the flexural behavior of normal strength concrete reinforced with coir under variation of the aspect ratio ($\lambda_f = l_f/d_f$) and dosage of the fibers compared to an unreinforced concrete (OC) in four-point bending tests. The flexural tensile strength as well as the post-crack behavior increased steadily with an increasing aspect ratio of the fibers and were maximum for coir with dimensions l_f/d_f = 75/0.25 mm. At 3.0% dosage of the fibers by weight of cement (wt% o.c.) (~12.7 kg/m^3), the maximum flexural tensile strength $f_{cflm,max}$ (= stress according to theory of elasticity at the lower edge of the beams when the maximum load F_{max} was reached) increased by 5% from 4.3 N/mm^2 (F_{max} = 11.3 kN) to 4.5 N/mm^2 (F_{max} = 11.8 kN). Regardless of the aspect ratio and the dosage of fibers, fiber pullout and thus failure occurred in the bond between the fibers and the cementitious matrix. Although this mode of failure is targeted to ensure ductile behavior [7,42], it also reveals that the tensile strength of the fibers is not fully utilized. Similar results were also obtained in the

studies by Pereira et al. [43], Ramli and Dawood [44], Hwang et al. [45], as well as Baruah and Talukdar [46].

In order to achieve a higher utilization of the tensile strength of the fibers, the aspect ratio of the fibers can be increased and thus a better bond can be achieved. However, with increasing slenderness, the fibers have a negative effect on the workability of the fresh concrete [7,47]. It should also be taken into account, that plant fibers absorb a part of the mixing water due to their hydrophilic behavior and thus further reduce the workability. In the investigations by Ali et al. [41], this led to a decrease in the flowability and compactability of the fresh concrete despite an increase in the water/cement ratio. It can be assumed that a further increase in the aspect ratio will further limit these, and thus the mechanical properties of the PFRC will be equally negatively affected.

Since an improvement of the bond by hooked-ends or profiling is (almost) impossible for plant fibers [48], the bond of plant fibers used in polymers is often improved by alkaline pretreatment of the fibers [36,49,50]. Similar positive effects on bonding have also been observed in studies of cementitious materials. In studies by Momoh et al. [51], alkaline pretreatment of oil palm broom fibers increased the mean transferable bond stress by 16% from 0.56 N/mm^2 to 0.65 N/mm^2 after 28 days. Yan et al. [17] investigated the flexural behavior of beams made of normal-strength concrete (with a compressive strength of 22.4 N/mm^2) and reinforced with 1.0 wt% o.c. (~3.1 kg/m^3) coir (l_f/d_f = 50/0.25 mm) using four-point bending tests. When untreated coirs were used, the maximum flexural tensile strength $f_{\text{cflm,max}}$ already increased by 14.2% from 9.8 N/mm^2 (F_{max} = 5.4 kN) to 11.2 N/mm^2 (F_{max} = 6.2 kN) compared to beams without fibers (OC), and when fibers with an alkaline pretreatment were used, it increased by another 6% to 11.9 N/mm^2 (F_{max} = 6.6 kN). The use of the fibers further prevented brittle failure of the bending beams and a certain post-crack tensile strength was observed after cracking. Figure 2 shows the load-deflection curves of the bending tests by Yan et al. [17]. Of particular note is the initial course of the curves, which can be attributed to slippage, settlements, etc., of the test facility. However, since this course makes it difficult to evaluate the post-crack tensile strength of the beams, the load F at a deflection δ of 0.4 mm (= $F_{0.4}$) and at a deflection δ of 3.4 mm (= $F_{3.4}$) is used in each case after the maximum load F_{max} has been reached. These then correspond approximately to the evaluation points according to EN 14651 [52] at a deflection of 0.5 mm and 3.5 mm or equivalent crack widths of 0.5 mm and 4.0 mm. For the bending beams reinforced with coir (PFRC), $F_{0.4}$ = 2.0 kN shows that 33.0% of the maximum load F_{max} (6.2 kN) can still be absorbed. With alkalized coir (alkalized PFRC), the load $F_{0.4}$ with 2.7 kN corresponds to 41.5% of the maximum load F_{max} and could thus be increased by 34.9% compared to the untreated coir. For the load $F_{3.4}$, it can be seen that the loads of the two test series converge and are approximately equal. The load $F_{3.4}$ for the beams with untreated coir (PFRC) still corresponds to 20.0% ($F_{3.4}$ = 1.2 kN) and for the beams with alkaline pretreated coir (alkalized PFRC) to 20.2% ($F_{3.4}$ = 1.3 kN) of the respective maximum load F_{max}. Consequently, the difference is only 7.9%.

Similar results were obtained by Ozerkan et al. [53] and Zhou et al. [54]. In the studies by Zhou et al. [54], although bond failure of the fibers still occurred primarily when alkalized fibers were used, fiber breakage was also observed.

When plant fibers are used in concretes, another problem arises in addition to the comparatively poor bond: the degradation in an alkaline environment. Although the cellulose fibers, which are decisive for the tensile strength, are relatively alkali-resistant compared to the other fiber components, prolonged exposure to an alkaline environment, as prevails in conventional concretes and mortars, leads to embrittlement and slow degradation of the cellulose fibers [18,21,55] as well as to a decrease in the transferable bond stress [51].

Degradation of plant fibers can be prevented by, inter alia, reducing the alkalinity of the concrete. John et al. [56], for instance, studied coir that had been embedded in a cement mortar with low alkalinity (pH = 10.3) for 12 years. No significant change in the chemical composition and structure of the fibers was observed. One way to limit alkalinity is to use pozzolans. Moreover, the reaction of the silica contained in the pozzolans with the

calcium hydroxide crystals (CH crystals)—present especially in the contact zone between the hydrated cement and the aggregates or fibers—to calcium silicate hydrate (CSH) phases improves the bond between the cementitious matrix and the fibers [1,57].
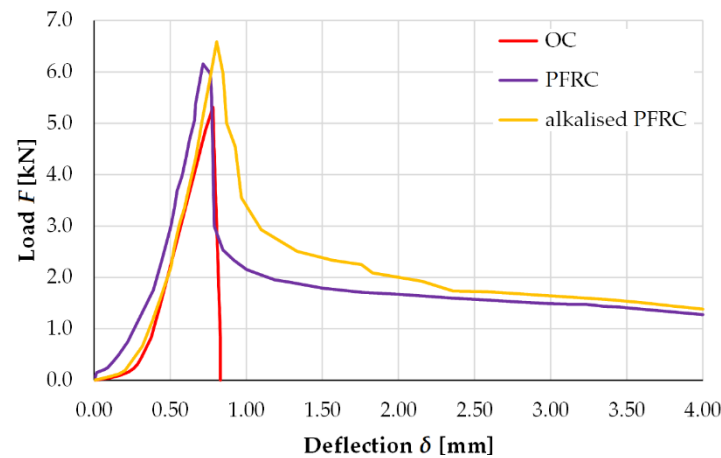

Figure 2. Typical load-deflection curves of bending beams made of unreinforced concrete (OC) and with a dosage of 1.0 wt% o.c. coir (PFRC) and alkalized coir (alkalized PFRC) reinforced concrete according to Yan et al. [17].

Ahmad et al. [58] used a concrete mix with a microsilica content of 52.5 kg/m^3 in their investigations (three-point bending tests) to determine the flexural strength of with coir reinforced concrete (with a compressive strength of 49 N/mm^2). Different dosages of fibers (0.5 wt% o.c. (~2.6 kg/m^3) to 2.0 wt% o.c. (~10.5 kg/m^3)) and different dimensions (l_f/d_f = 25/0.32 mm, 50/0.32 mm and 75/0.32 mm) were used. Both the maximum flexural tensile strength $f_{cflm,max}$ and the load that can be applied after cracking tended to increase with an increasing aspect ratio of the fibers λ_f. At a dosage of fibers of 1.5 wt% o.c. (~7.9 kg/m^3) with dimensions of the fibers of l_f/d_f = 75/0.32 mm, the maximum flexural tensile strength $f_{cflm,max}$ increased by 6% from 6.35 N/mm^2 (F_{max} = 10.3 kN) to 6.61 N/mm^2 (F_{max} = 11.0 kN) compared to an unreinforced concrete (OC). In the post-cracking stage, the load $F_{0.4}$ with 1.2 kN was 10.5% of the maximum load F_{max} and the load $F_{3.4}$ with 0.9 kN was 7.9% of the maximum load F_{max}. A further increase in the dosage of fibers up to 2.0 wt.% o.c. (~10.5 kg/m^3) improved the post-crack behavior and increased the load $F_{0.4}$ by 119% to 2.5 kN and $F_{3.4}$ by 108% to 1.8 kN, but at the same time resulted in a poorer workability of the fresh concrete as well as a reduction in the maximum flexural strength $f_{cflm,max}$ by 11% to 5.87 N/mm^2 and of the maximum load F_{max} by 11% to 9.9 kN (see Figure 3).
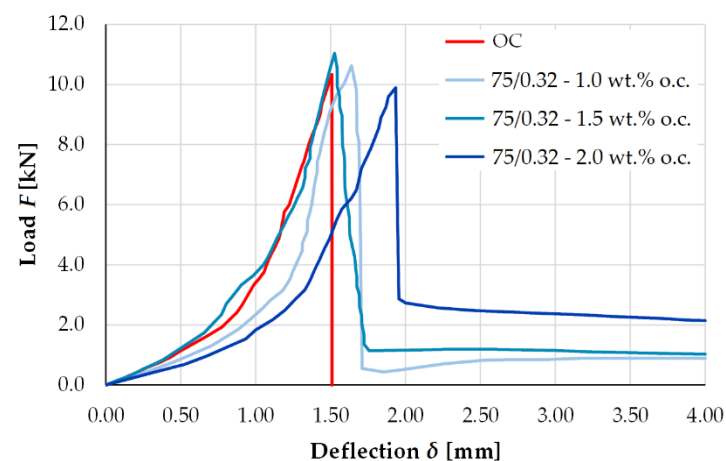

Figure 3. Load-deflection curves of bending beams made of unreinforced concrete (OC) and of coir reinforced concrete with different dosages of fibers according to Ahmad et al. [58].

Despite the long fiber length of 75 mm and the improved contact zone due to the use of pozzolans, the investigations of Ahmad et al. [58] still showed a bond failure of the fibers and in part poorer mechanical properties of the PFRC, so that it can be concluded that the fibers are not properly utilized. A further increase in fiber length would likely further limit the workability of the fresh concrete and thus the load-bearing behavior of the PFRC. Although the workability could be improved by increasing the water percentage [41], this generally decreases the mechanical properties of the concrete [59]. In addition, plant fibers absorb some of the mixing water due to their hygroscopic properties, which leads to an increase in the volume of the fibers (primary swelling) during concreting. After the concrete hardens, the fibers dry, which leads to a reduction in the volume of the fibers and thus to a weakening of the bond between the concrete and the fibers [47,60–62]. This effect can also be caused by secondary swelling or drying of the plant fibers in the hardened concrete due to fluctuating pore moisture [18,31,63]. In order to reduce the swelling of natural fibers in concrete, a reduction in the water/cement ratio with a simultaneous optimization of the contact zone between fiber and concrete (improved bond) as well as a higher impermeability of the concrete should be aimed for. Ultra-high performance concrete (UHPC) represents a material optimized in this respect.

2.3. Ultra-High Performance Fiber-Reinforced Concrete

Ultra-high performance concretes are characterized by their high compressive strength of about 150 to 200 N/mm^2 [1]. This high load-bearing capacity is achieved by minimizing microstructural disturbances and increasing the packing density, which is achieved in particular by a grain size distribution optimized up to the fine grain range, a strong reduction in the water/cement ratio to 0.25 to 0.15 and the use of inert and reactive additives [59,64]. Due to the high silica content as well as the high relative surface area and the associated high reactivity, micro- or nanosilica are commonly used here. The high mass fraction of pozzolans, often up to 30 wt.% o.c., leads to a transformation of the entire free calcium hydroxide and thus to a reduction in the alkalinity to a pH value below 10 [65].

A pH value of 10 can lead to depassivation of the steel surface in the case of steel reinforcement [65]. However, due to the optimized microstructure and the resulting high impermeability, transport processes are almost completely suppressed in UHPC, so that even with a minimum concrete cover, no water necessary for steel corrosion reaches the reinforcement and thus a high durability is achieved [1,66–68].

As a result of the reduced requirements for concrete cover and the high performance of UHPC (especially very high compressive strength and durability), extremely thin-walled and thus resource-optimized components and structures can be built with UHPC [69,70], so that they have a higher sustainability than those made of normal strength concretes [71–74].

However, a disadvantage of UHPC is its brittle failure under compressive loading. For this reason, micro steel fibers are almost always added to UHPC, which has a enormous influence on the ductility of the ultra-high performance steel fiber-reinforced concrete (UHPFRC) [69,75]. Due to the use of high contents of pozzolans, the low water/cement ratio and the optimized packing density, UHPC has a significantly improved contact zone compared to normal strength concretes. As a result, even with straight, smooth, high-strength steel fibers without hooked-ends or profiling and an aspect ratio λ_f of 60 to 100, no further measures are necessary to ensure a sufficient bond between the fibers and the surrounding cementitious matrix [7]. Additional anchoring by using hooked-ends or profiling would be more likely to lead to fiber breakage and thus to detrimental brittle failure of the concrete element [42,76].

However, the steel fibers not only increase the ductility under compressive loading, but also the toughness under tensile loading due to a high post-crack tensile strength. The high post-crack tensile strength of the UHPFRC can, among other things, lead to a reduction in the required reinforcing steel reinforcement bars. However, it should also be noted at this point that micro steel fibers negatively affect the sustainability of the UHPFRC [72].

This could be remedied, for example, by the use of plant fibers. However, as far as the authors are aware, no studies have yet been carried out on the use of plant fibers in UHPC.

2.4. Summary and Conclusions of the State of Research

The use of natural plant fibers can improve the load-bearing behavior of cementitious materials both in the non-cracked and cracked state, e.g., by increasing the flexural strength and toughness (post-crack tensile strength). However, the positive influence of the fibers on the load-bearing behavior is limited when normal-strength concrete is used due to the comparatively poor bond and the swelling capacity of the fibers. In addition, the high alkalinity of the concrete with a pH $\geq$ 12 attacks the plant fibers, causing them to become brittle and degrade over time.

These disadvantages could most likely be minimized or even completely avoided by using UHPC. Due to the low alkalinity and the high impermeability of UHPC, sufficient durability of the plant fibers could be ensured, and due to the very good bond, the integration and thus the load-bearing capacity of the fibers in the concrete could be significantly improved. At the same time, the fibers could in turn further improve the ductility and toughness of the otherwise brittle material as well as the sustainability of the UHPC. As a natural plant fiber source, bamboo is particularly promising. It is locally and inexpensively available in many regions of the world (see Figure 1), grows very rapidly [77], and has promising mechanical properties (see Table 1). Since no studies on ultra-high performance plant fiber-reinforced concrete (UHPPFRC) are available so far, first experimental investigations on the flexural behavior of bamboo fiber-reinforced UHPC have been carried out at the Institute of Concrete Construction (IfMa) of Leibniz University Hannover, which will be reported below.

3. Experimental Investigations

3.1. Test Specimen

The experimental investigations were carried out in accordance with the DAfStb guideline for "Steel Fiber Reinforced Concrete" [42,78] using unnotched four-point bending tests. The bending beams had a span of 600 mm and a width and height of 150 mm each. The fresh concrete was placed in the formwork from one end face and was compacted by using a vibrator. Immediately after concreting, the bending beams were covered with a foil, stripped of their formwork after two days and then stored under foil in a climatic chamber at a room temperature of 20°C ($\pm$2°C) and a relative humidity of 65% ($\pm$5%) until testing.

The ultra-high performance concrete used was the fine-grain mix RU1 of the DFG priority program SPP 2020 [79–81] with an average axial compressive strength of 160 N/mm^2. Straight bamboo fibers with dimensions l_f/d_f = 30/0.5 mm were added to the UHPC in a dosage of 0.00 wt% o.c. (0.0 kg/m^3), 1.25 wt% o.c. (9.6 kg/m^3), and 2.50 wt% o.c. (19.2 kg/m^3). To ensure adequate flowability of the bamboo fiber-reinforced UHPC, the dosage of superplasticizer was increased by 50% for the ultra-high performance plant fiber-reinforced concretes. The UHPC mixes used can be found in Table 2 and the fresh concrete properties of the UHPC mixes, which were determined directly after the mixing process—within 12 min—can be found in Table 3.

The bamboo fibers used in the studies were mechanically extracted from the culm wall of a Moso bamboo (latin name: Arundinarieae Arundinariinae Phyllostachys Pubescens). For this purpose, the internodes of a culm were divided into splits of about 50 mm in width. After soaking the splits in water, they were cut into slices about 0.6 mm thick, and—due to the higher tensile strength in the outer half [82]—only the slices obtained from the outer two-thirds of the splits were further processed. After soaking in water again and cutting into 3 cm long segments, these were cut into 0.6 cm wide fibers in the final mechanical processing step and subsequently air dried. The performed steps of fiber extraction are shown in Table 4 as well as Figure 4.

Table 2. UHPC mixtures in [kg/m^3].

Components	UHPC	UHPPFRC-F1.25	UHPPFRC-F2.50
CEM I 52.5 R-SR3/NA (Holcim Sulfo 5R)	786.2	771.8	766.8
Silica fume (Sika® Silicoll P (uncompacted))	166.7	163.6	162.6
Quartz powder (Quarzwerke MILLSIL® W12)	196.1	192.5	191.3
Quartz sand (0/0.5 mm) (Quarzwerke H33)	959.8	942.2	936.1
Superplasticiser (BASF MasterGlenium® ACE 394)	24.1	35.1	34.9
Water	185.7	182.3	181.2
Bamboo Fiber ($l_f/d_f = 30.0/0.5$ mm)	0.0	9.6	19.2

Table 3. Fresh concrete properties of the UHPC mixtures.

Characteristic	UHPC	UHPPFRC-F1.25	UHPPFRC-F1.25
Temperature of fresh concrete [°C]	24.0 ± 1.0		
Slump-flow measure (without locking ring) [mm]	735	820	715
Air content [%]	4.1	4.2	4.3
Density [kg/m^3]	2270	2257	2240

Table 4. Steps of fiber extraction.

No.	Name	Description
1	Divide I	Divide the bamboo culm into nodes and internodes
2	Split	Split internodes into 50 mm wide splits
3	Soaking I	Soak splits for 3 days
4	Planing	Divide the splits into slices with a hand plane
5	Soaking II	Soak slices for 1 day
6	Divide II	Cut the slices into segments with tin snips
7	Separation	Separate the fibres from the segments with a carpet knife
8	Drying	Air-dry the obtained fibres for one week
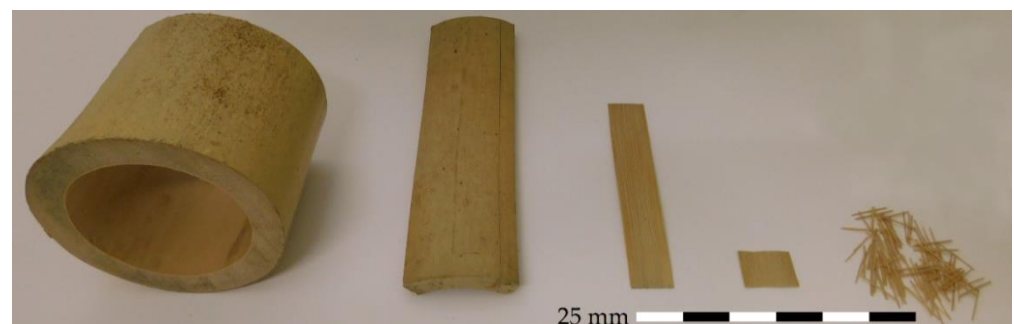
Figure 4. Essential steps of fiber extraction (from left to right: separated internode; slits; slices; segments; fibers).

The test program included a total of nine bending beams under a variation of the dosages of fibers (Table 5).

Table 5. Test program.

Series	UHPC Mixture	Dosage of the Fibers [wt% o.c.]	Number of Specimens
B-F0.00	UHPC	0.00	3
B-F1.25	UHPPFRC-F1.25	1.25	3
B-F2.50	UHPPFRC-F2.50	2.50	3

3.2. Test Setup and Execution

The test setup, the test facility and the measurement technology used (Figure 5) were based on [42,83]. In order to record the post-crack behavior, the tests were deformation-controlled according to the underlying guideline. The applied load F and the deflection δ were continuously measured and recorded. In addition, strain gauges (SG) were applied to one bending beam of each series (B-F0.00, B-F1.25 and B-F2.50) in the center of the field on the side faces (both sides) at three height positions. In order to ensure as uniform a surface as possible in the area of the SG, the bending beams were tested in such a way that the concreting side represented the top side of the bending beams.
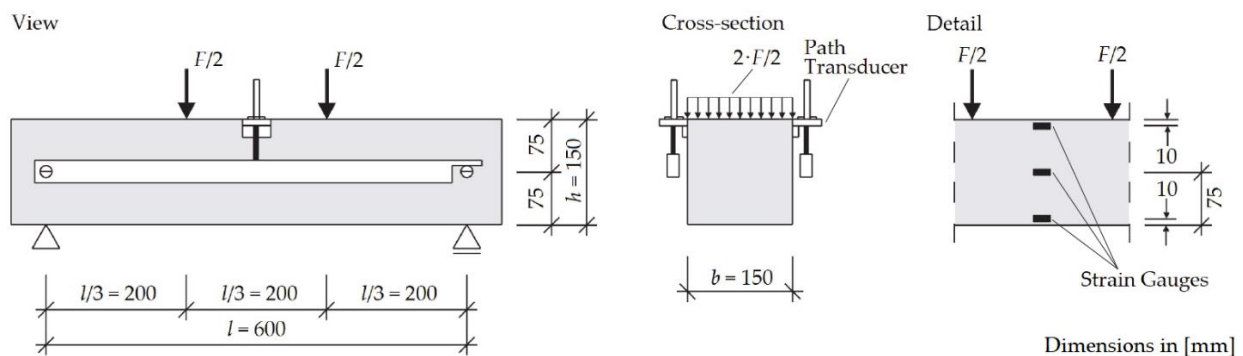

Figure 5. Test setup of the four-point bending test on the basis of [42,78].

3.3. Experimental Results

As expected, brittle failure occurred during testing of the bending beams without bamboo fibers, whereas ductile cracking behavior occurred during the tests with bamboo fibers. Figure 6 shows the crack pattern of the bending beams after the tests were carried out comparatively with a 0.00 wt.% o.c., 1.25 wt.% o.c. and 2.50 wt.% o.c. dosage of bamboo fibers. The crack pattern in all tests was characterized by a main crack with fiber pullout without a multiple crack formation. Figure 7 shows a close-up of the failure crack of test B-F2.50-2, which clearly shows the crack-bridging effect of the bamboo fibers across the crack.

The load-deflection curves of the individual test series up to a deflection δ of 0.10 mm can be seen in Figure 8. Here, the dotted lines of each color represent the individual results and the solid lines represent the average load of the test series at a given deflection. It can be seen that the curves of the bending beams without bamboo fibers (B-F0.00) show a linear progression until reaching the maximum load F_{max} of 19.5 kN on average and fail brittly after a minimum load drop (elastic limit). The curves of the fiber-reinforced bending beams show a higher maximum load F_{max} compared to those of the plain bending beams. Thus, the average ultimate load F_{max} of the test series B-F1.25 with 26.8 kN exceeds that of the unreinforced bending beams by 37.1% and that of the test series B-F2.50 with 25.6 kN exceeds that of the unreinforced bending beams by 31.3%. In the case of B-F2.50, however, the mean value of the test series is strongly reduced by the low load-bearing capacity of one bending beam, which, at 19.0 kN, has a maximum load similar to that of

the unreinforced beams. The lower load-bearing capacity of this beam could therefore be due to an unexpected and undesirable absence of fibers in the cracked cross-section. Neglecting this beam, the mean value of the maximum load corresponds to $F_{max} = 28.9$ kN, which is 48.2% more than for the flexural beams without fiber reinforcement. As with the unreinforced beams, the curves of the fiber-reinforced flexural beams are largely linear until the maximum load is reached. In some cases, however, there is a brief drop in stiffness and an increase in deflection in the upper 1/3 of the load (cf. I in Figure 8). In some cases, there is also a significant drop in stiffness before the maximum load is reached (cf. II in Figure 8).

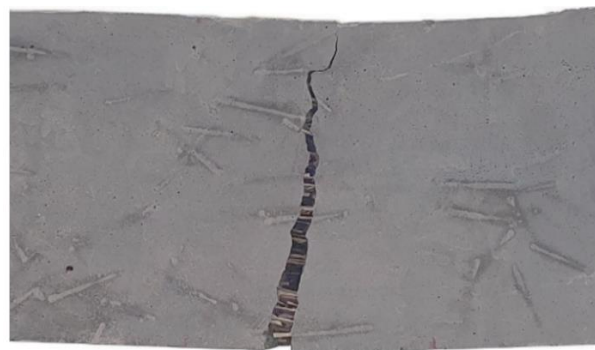**Figure 6.** Crack patterns after the test (side view).

Figure 7. Detail of the failure crack of test B-F2.50-2.
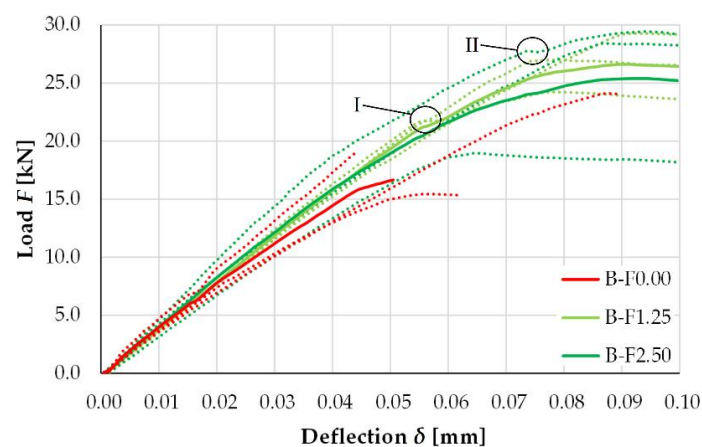

Figure 8. Load-deflection curves of the bending beam tests up to a deflection of $\delta = 0.1$ mm with drop of the stiffness (detail I and II).

The curves of the strain ε (mean values) measured by the SG and the curves of the load F both as a function of the deflection δ of the bending beams with the applied strain gauges of the test series B-F0.00, B-F1.25 and B-F2.50 are shown in Figure 9. For the bending beam without fiber reinforcement (B-F0.00), the measured strain near the bottom and top edges (SG_b and SG_t) increases linearly up to $|0.065‰|$ up to the maximum load, while the strain in the beam center (SG_m) remains constant at 0‰. The strain curves of the specimen with a dosage of fibers of 1.25 wt% o.c. (B-F1.25) show a similar course until cracking (cf. cross in Figure 9), where the maximum measured strain of 0.084‰ (mean value) before reaching the elastic limit exceeds the maximum strain value for the bending beam without fiber reinforcement by 29.2%. Although the load curve of the beam without fiber reinforcement ends with the crack formation ($F_{crack} = F_{max} = 19.1$ kN), the curve of the specimen with a dosage of fibers of 1.25 wt.% o.c. (B-F1.25) increases over the crack formation ($F_{crack} = 21.5$ kN) to a maximum load of $F_{max} = 24.2$ kN (cf. triangle in Figure 9). With the crack formation, there is also an elongation in the center of the beam (SG_m). The strain curve of the upper strain gauge SG_t continues to increase linearly in this region and is approximately 0.130‰ at the time of maximum load. For the strain curve of SG_b, only the data up to F_{crack} are available, since the SG near the bottom edges failed with the crack formation. The strain curves of the bending beam with a dosage of fibers of 2.50 wt.% o.c. (B-F2.50) show a comparable linear or constant course as the other beams in the uncracked stage up to a strain of approx. 0.075‰ (mean value). However, with further increasing deflection, there are strong deviations from this curve progression. As the load-deflection curve flattens, there is also a reduced increase in compression strain near the top of the beam (SG_t) and a reduced increase in strain near the bottom of the beam (SG_b), while there is an increase in strain in the beam center (SG_m). Thereby, the strain rate in the lower layer decreases more than the compression strain rate at the upper edge, which can be explained by the rise of the neutral axis in the cracked sections. With the crack formation at a strain of 0.116‰ ($F_{crack} = 27.8$ kN), there is a further flattening of the SG_b curve, whereas the strain in the middle center SG_m increases slightly. The maximum strain of SG_b of 0.125‰, which is reached at a maximum load of $F_{max} = 29.4$ kN, exceeds that of the bending beam without fiber reinforcement by 89.1% (Figure 9).

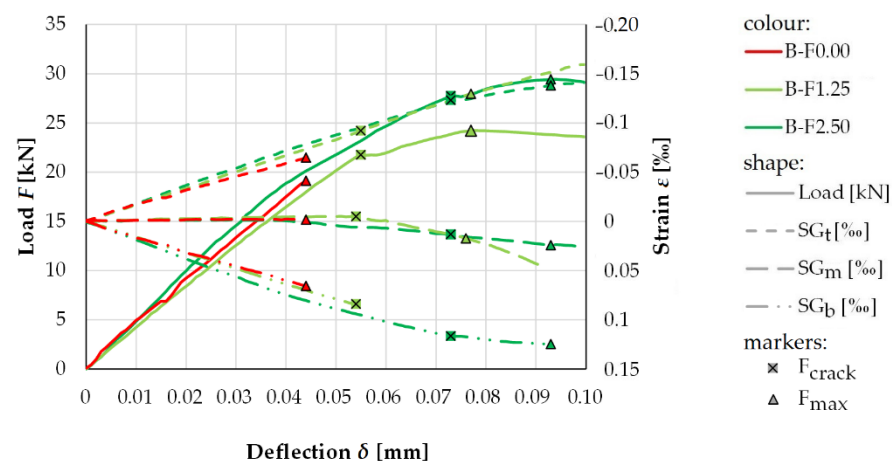**Figure 9.** Load-deflection curves (Load F) and mean values of strain ε measured with strain gauges in upper (SG_t), middle (SG_m), and lower (SG_b) positions of bending beams with a dosage of 0.00 wt% o.c. (B-F0.00), 1.25 wt% o.c. (B-F1.25), and 2.50 wt.% o.c. (B-F2.50) bamboo fibers up to a deflection of $\delta = 0.1$ mm.

The load-deflection curves of the individual tests or series up to a deflection δ of 4.00 mm can be taken from Figure 10. The dotted lines of each color again represent the individual results and the solid lines again represent the average value of the test series (cf. Figure 8). In the case of the fiber-reinforced beams, the load F decreases slowly with increasing deflection after cracking of the cross-section (deflection-softening [84]), and the

bamboo fibers are able to prevent brittle failure of the UHPC. Here, the load F decreases faster for the bending beams B-F1.25 with a dosage of fibers of 1.25 wt% o.c. (9.6 kg/m^3) than for the bending beams B-F2.50 with a dosage of fibers of 2.50 wt% o.c. (19.2 kg/m^3). At a post-crack-deflection δ of 0.4 mm, the load $F_{0.4}$ of test series B-F2.50, 13.6 kN, exceeds that of test series B F1.25 (11.2 kN) by 21.3%. At a post-crack-deflection of 3.4 mm, $F_{3.4}$ of B-F2.50 with 7.1 kN exceeds that of test series B-F1.25 by 60.7% (4.4 kN) (Figure 10). Due to the crack-bridging effect of the bamboo fibers, 41.9% (B-F1.25), respectively, 53.3% (B-F2.50) of the maximum load could still be transferred at a post-crack-deflection of 0.4 mm, and 16.3% (B-F1.25), respectively, and 27.3% (B-F2.50) at a further deflection of 3.4 mm after crack formation. Table 6 gives an overview of the relevant test results.
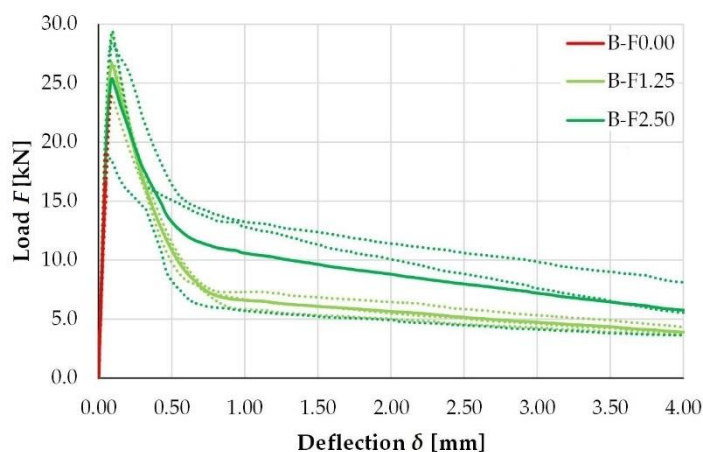

Figure 10. Load-deflection curves of the bending beam tests up to a deflection of δ = 4.0 mm.

Table 6. Overview of the mean value of the decisive test results and the maximum deviation from the mean values (=value inside the brackets).

Series	Maximum Load $F_{\max}$ [kN]	Strain When Reaching the Maximum Load ε_{max} [‰]	Load $F_{0.4}$ [kN]	Load $F_{3.4}$ [kN]
B-F0.00	19.5 ($\pm$4.5)	0.065	-	-
B-F1.25	26.8 ($\pm$2.6)	0.084	11.3 ($\pm$1.2)	4.4 ($\pm$0.6)
B-F2.50	25.6 ($\pm$6.6)	0.125	13.6 ($\pm$4.6)	7.0 ($\pm$3.6)

4. Discussion and Comparison of the Results

The use of bamboo fibers in UHPC significantly increased both the maximum load $F_{\max}$ and the strain $\varepsilon_{\max}$ when reaching the maximum load in the experimental investigations. It can therefore be assumed that the bamboo fibers bridge the microcracks already present in the uncracked state and thereby delay the formation of the macrocrack (Figures 8 and 9).

The use of bamboo fibers also improved the post-crack behavior of the UPHC and prevented brittle failure of the bending beams (Figures 6, 7 and 10). Here, both the bending beams with 1.25 wt% o.c. (9.6 kg/m^3) and those with 2.50 wt% o.c. (19.2 kg/m^3) bamboo fibers showed a deflection-softening material behavior (Figure 9). However, in the case of the B-F2.50 series bending beam applied with strain gauges, a deviation from the otherwise linear course of the strain curves was observed in the upper third of the maximum load. The increase in the tensile zone and the drop in stiffness of the bending beams before the maximum load was achieved (cf. I and II in Figure 8) indicates that a slow opening of the failure cracks already occurred in the lower beam region, but the bamboo fibers were able to prevent a sudden rupture of the cross-section. Consequently, it can be concluded for the post-cracking stage that the bamboo fibers bridge the cracks that occur and allow load transfer across the crack edges (=crack-bridging effect).

In order to examine this effect, respectively, and the post-cracking load-bearing capacity further, a comparison of the own tests with the bending beams according to Yan et al. [17] (Figure 2) and Ahmad et al. [58] (Figure 3) is made below. At this point, however, it should be pointed out that a comparison is only possible to a very limited extent due to the different test execution (three-point bending test vs. four-point bending test) and also concrete properties (normal-strength concrete vs. UHPC). However, since there are no comparable tests in the literature so far, the tests according to Yan et al. [17] and Ahmad et al. [58] are used here. Figure 11 shows the average value of the load-deflection curves after reaching the maximum load F_{max} of the test series B-F1.25 with a dosage of 1.25 wt% o.c. (9.6 kg/m^3) and B-F2.50 with a dosage of 2.50 wt% o.c. (19.2 kg/m^3) bamboo fibers in comparison with the load-deflection curves of the beams tested by Ahmad et al. [58] and Yan et al. [17] (see Section 2.2). The maximum load of the bamboo fiber-reinforced bending beams B-F1.25 (26.8 kN) and B-F2.50 (25.6 kN) exceeds that of the 2.0 wt.% o.c. (~10.5 kg/m^3) coir-reinforced bending beams of Ahmad et al. [58] (9.9 kN) and that of the 1.0 wt.% o.c. (~3.1 kg/m^3) alkalized coir-reinforced bending beams of Yan et al. [17] (6.6 kN) significantly. The load after cracking (post-crack behavior) for tests B-F1.25 and B-F2.50 is also higher than those of Ahmad et al. [58] and Yan et al. [17]. Therefore, $F_{0.4}$ for the UHPPFRC bending beams is 11.2 kN (B-F1.25) and 13.6 kN (B-F2.50), respectively; whereas, the considered bending beam of Ahmad et al. [58] with 2.5 kN has only 22.4% or 18.5% of the post-crack load-bearing capacity of the bamboo fiber-reinforced UHPC bending beams. The load-deflection curve of the bending beam by Yan et al. [17] shows a similar low test load of 2.0 kN (18.0% or 14.9%) for $F_{0.4}$ compared to the UHPPFRC bending beams as that of Ahmad et al. [58]. As the test progresses, the absorbable load of the bending beam of Yan et al. [17] drops below that of Ahmad et al. [58] and, at a post-crack-deflection δ_C of 3.4 mm, equals 1.3 kN, which is 73.5% of the latter; the test load of the UHPPFRC bending beams, however, remain significantly higher than in the tests with coir-reinforced bending beams made of normal-strength concrete, at 4.4 kN and 7.0 kN, respectively.
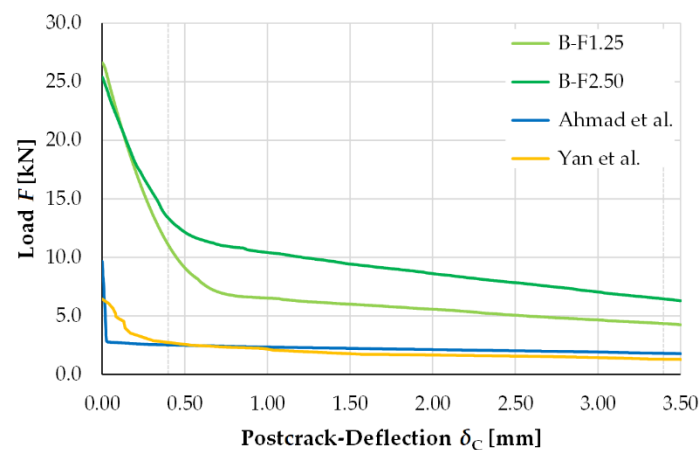

Figure 11. Load-deflection curves of the bending beams with 1.25 wt.% o.c. (9.6 kg/m^3; B-F1.25) and 2.5 wt.% o.c. (19.2 kg/m^3; B-F2.50) bamboo fibers and with 2.0 wt.% o.c. (~10.5 kg/m^3) coir of dimensions l_f/d_f = 75/0.32 mm according to Ahmad et al. [58] and with 1.0 wt.% o.c. (~3.1 kg/m^3) alkalized coir of dimensions l_f/d_f = 50/0.25 mm according to Yan et al. [17].

In the case of the bending beams reinforced with coir or alkalised coir, it must be considered that the fibers will most likely degrade over time in the alkaline environment of the normal-strength concrete and that their performance will thus decrease, especially in the post-cracking stage. Furthermore, a reduction in the performance due to a reduction in the bond by secondary swelling of the fibers due to the low impermeability of the normal strength concrete compared to UHPC has to be considered.

As these effects (most likely) do not occur with the combination of bamboo fibers and UHPC and a very high performance can be achieved, bamboo fiber-reinforced UHPC has

an enormous potential with regard to the worldwide production of extremely thin-walled, resource-saving, environmentally friendly and sustainable components and structures.

5. Conclusions and Suggestions for Future Research

The load-bearing behavior of concretes can be improved by using fibers. Plant fibers represent a sustainable alternative to synthetic fibers such as steel fibers, which are often used conventionally. The knowledge gained in this paper are as follows:

1. Bamboo fibers have the potential to become a sustainable alternative to conventional steel fibers, especially in view of the worldwide distribution and cultivation possibilities, the rapid growth, the simple harvesting and processing, as well as the very good mechanical properties of bamboo (Table 1 and Figure 1).

2. In experimental investigations already carried out, the use of plant fibers prevented the brittle failure of concrete subjected to bending stress and achieved ductile behavior. However, the load-bearing capacity of the plant fiber-reinforced concrete was limited, in particular, by the poor bond between the fibers. In addition, corrosion in the alkaline environment of the concrete and the swelling behavior of the fibers pose a fundamental problem.

3. Ultra-high performance concretes (UHPC) are characterized by, among other things, low alkalinity, high impermeability, low water/cement ratio, and very good bonding, and thus could overcome the problems mentioned in point 2 that exist with the use of plant fibers in cementitious materials. Furthermore, UHPC can be used to produce very thin-walled and thus resource-optimized and sustainable components and structures.

4. The use of 1.25 wt.% o.c. (9.6 kg/m^3) and 2.50 wt.% o.c. (19.2 kg/m^3) bamboo fibers bridged existing microcracks and delayed macrocrack formation in the experimental tests conducted on UHPC bending beams. As a result, the maximum load could be increased by 37.1% and 30.9% (48.2%) from 19.5 kN to 26.8 kN and 25.6 kN (28.9 kN), respectively (Figure 8).

5. The bamboo fibers were able to prevent the brittle failure of the UHPC and ensure ductile behavior by the crack-bridging effect. With deflection-softening behavior, the beams with a dosage of fibers of 1.25 wt.% o.c. (9.6 kg/m^3) were capable of 11.3 kN (42.5% of the maximum load F_{max}) at a post-crack deflection of 0.4 mm, and at a post-crack deflection of 3.4 mm, 4.4 kN (16.4% of F_{max}), whereas the bending beams with a dosage of fibers of 2.50 wt.% o.c. (19.2 kg/m^3) could support 13.6 kN (53.3% of F_{max}) and 7.0 kN (27.3% of F_{max}), respectively (Figure 10).

6. A comparison of the post-cracking behavior of the own bending tests with those of the literature, which were carried out on normal-strength concretes reinforced with (alkalised) coir, clearly shows that a significant improvement of the load-bearing and deflection behavior in the cracked state can be achieved by a combination of bamboo fibers and UHPC (Figure 11).

The experimental investigations carried out clearly show the enormous potential of the combination of bamboo fibers and UHPC, which can for example lead to thin-walled, material-optimized and thus extremely sustainable structural components. However, the performed tests are limited to only nine specimens, in which the load-bearing performance was investigated based on two dosages of bamboo fibers (1.25 wt.% o.c. and 2.50 wt.% o.c.) in comparison with a plain UHPC. In order to better understand the durability and the mechanical properties of bamboo fiber-reinforced UHPC, further experimental investigations need to be carried out, looking at, among other things, the durability of bamboo fibers in UHPC and the load-bearing behavior under a variation of concrete mix, aspect ratio and other dosages of fibers. In addition, sustainability can be further improved by using an ecologically optimized UHPC, a so-called Green Ultra-High Performance Concrete [85,86].

Furthermore, bamboo has the potential to further improve the mechanical properties and sustainability of UHPC when used as whole culms or strips and thus as reinforcement

bar. Test specimens made of UHPC reinforced with bamboo culms as well as bamboo culms and bamboo fibers have already been produced at the Institute of Concrete Construction (IfMa) of Leibniz University Hannover and are to be tested soon. This will be reported on at a later date.

References

1. German Committee for Structural Concrete. *Sachstandsbericht Ultrahochfester Beton—Betontechnik und Bemessung (DAfStb-Issue 561)*; Beuth Publishing: Berlin, Germany, 2008; ISBN 978-3-410-65045-4.
2. Tiberti, G.; Germano, F.; Mudadu, A.; Plizzari, G. An overview of the flexural post-cracking behavior of steel fiber reinforced concrete. *Struct. Concr.* **2017**, *19*, 695–718. [CrossRef]
3. Conforti, A.; Zerbino, R.; Plizzari, G. Influence of steel, glass and polymer fibers on the cracking behavior of reinforced concrete beams under flexure. *Struct. Concr.* **2018**, *20*, 133–143. [CrossRef]
4. Oettel, V.; Schulz, M.; Haist, M. Empirical approach for the residual flexural tensile strength of steel fiber-reinforced concrete based on notched three-point bending tests. *Struct. Concr.* **2022**, *23*, 993–1004. [CrossRef]
5. Empelmann, M.; Oettel, V.; Cramer, J. Berechnung der Rissbreite von mit Stahlfasern und Betonstahl bewehrten Betonbauteilen. *Beton-Und Stahlbetonbau* **2020**, *115*, 136–145. [CrossRef]
6. Oettel, V. Steel Fiber Reinforced RC Beams in Pure Torsion—Load-Bearing Behaviour and Modified Space Truss Model. *Struct. Concr.* **2022**. [CrossRef]
7. Holschemacher, K.; Dehn, F.; Müller, T.; Lobisch, F. Grundlagen des Faserbetons. In *Beton-Kalender 2017: Spannbeton, Spezialbetone*; Ernst & Sohn: Hoboken, NJ, USA, 2017; pp. 382–472. [CrossRef]
8. Destrée, X. Steel-Fibre-Reinforced Concrete elevated suspended Slabs: Design cases in Europe and the USA. In *Joint ACI-FIB International Workshop Fibre-Reinforced-Concrete: From Design to Structural Applications*; FRC: Lausanne, Switzerland, 2016. [CrossRef]
9. Hammond, G.; Jones, C. *Embobdied Carbon—The Inventory of Carbon and Energy (BSRIA)*; University of Bath: Bath, UK, 2010; ISBN 978-0-86022-703-8.
10. Kotaro, K.; Kaito, S. Environmental impact of carbon fibers fabricated by an innovative manufacturing process on life cycle greenhouse gas emissions. *Sustain. Mater. Technol.* **2022**, *31*, e00365. [CrossRef]
11. Hebel, D.E.; Heisel, F.; Javadian, A. Bambus statt Stahl. *Betonexperimente—TEC21* **2013**, *35*, 36–40. [CrossRef]
12. Hebel, D.E. Bamboo could turn the world. *ECOS* **2014**, *199*, 1–3. [CrossRef]
13. Hebel, D.E.; Heisel, F. *Fiber Composite Reinforced Concrete—A Material Research, Tropical Zone Worldwide*; Future Cities Laboratory (FCL): Singapore, 2013.
14. Das, S.; Warren, J.; West, D.; Schexnayder, S.M. *Global Carbon Fiber Composites Supply Chain Competitiveness Analysis*; Clean Energy Manufacturing Analysis Center: Denver, CO, USA, 2016.
15. Grand View Research. *Glass Fiber Reinforced Concrete Market Size, Share & Trends Analysis Report By Process*; Grand View Research: San Francisco, CA, USA, 2020.
16. Wagenführ, A. Naturfaserverbunde im Leichtbau. *Lightweight Des.* **2017**, *10*, 3. [CrossRef]
17. Yan, L.; Chouw, N.; Huang, L.; Kasel, B. Effect of alkali treatment on microstructure and mechanical properties of coir fibres, coir fibre reinforced-polymer composites and reinforced-cementitious composites. *Constr. Build. Mater.* **2016**, *112*, 168–182. [CrossRef]
18. Archila, H.; Kaminski, S.; Trujillo, D.; Escamilla, E.Z.; Harries, K.A. Bamboo reinforced concrete: A critical review. *Mater. Struct.* **2018**, *51*, 102. [CrossRef]
19. Kesikidou, F.; Stefanidou, M. Natural fiber-reinforced mortars. *J. Build. Eng.* **2019**, *25*, 100786. [CrossRef]
20. Franck, R.R. *Bast and Other Plant Fibres*; Elsevier, B.V.: Amsterdam, The Netherlands, 2005; ISBN 978-1-85573-684-9.

21. Mwaikambo, L.Y.; Ansell, M.P. Mechanical properties of alkali treated plant fibres and their potential as reinforcement materials. I. hemp fibres. *J. Mater. Sci.* **2006**, *41*, 2483–2496. [CrossRef]

22. Azwa, Z.N.; Yousif, B.F.; Manalo, A.C.; Karunasena, W. A review on the degradability of polymeric composites based on natural fibres. *Mater. Des.* **2013**, *47*, 424–442. [CrossRef]

23. Mwaikambo, L.Y.; Ansell, M.P. Mechanical properties of alkali treated plant fibres and their potential as reinforcement materials II. Sisal fibres. *J. Mater. Sci.* **2006**, *41*, 2497–2508. [CrossRef]

24. Chokshi, S.; Parmar, V.; Gohil, P.; Chaudhary, V. Chemical Composition and Mechanical Properties of Natural Fibers. *J. Nat. Fibers* **2020**, *19*, 3942–3953. [CrossRef]

25. Hebel, D.E.; Heisel, F.; Javadian, A. *Engineering Bamboo: Composite Fiber Materials as an Alternative Reinforcement in Structural Concrete Applications*; Future Cities Laboratory (FCL): Singapore, 2013; pp. 46–59. [CrossRef]

26. Canavan, S.; Richardson, D.M.; Visser, V.; le Roux, J.J.; Vorontsova, M.S.; Wilson, J.R. The global distribution of bamboos: Assessing correlates of introduction and invasion. *AoB PLANTS* **2017**, *9*, plw078. [CrossRef]

27. Javadian, A.; Smith, I.F.C.; Hebel, D.E. Application of Sustainable Bamboo-Based Composite Reinforcement in Structural-Concrete Beams: Design and Evaluation. *Materials* **2020**, *13*, 696. [CrossRef]

28. Lomelí-Ramírez, M.G.; Anda, R.R.; Satyanarayana, K.G.; de Muniz, G.I.; Iwakiri, S. Comparative Study of the Characteristics of Green and Brown Coconut Fibers for Development of Green Composites. *Bio Resour.* **2018**, *13*, 1637–1660. [CrossRef]

29. Lu, X.-S.; Wang, K.-Q.; Yi, X.-C.; Liou, J.; He, J.-X. A study on the physico-mechanical properties of culmwood of Phyll. glauca of Shandong. *J. Bamboo Res.* **1985**, *4*, 98–106.

30. Huang, Y.-H.; Fei, B.-H.; Yu, Y.; Zhao, R.-J. Plant age effect on mechanical properties of Moso bamboo (*Phyllostachys heterocycla* var. *Pubescens*) single fibers. *Wood Fiber Sci.* **2012**, *44*, 196–201.

31. Hidalgo-Lopez, O. *Bamboo—The Gift of the Gods*; O. Hidalgo-Lopez: Bogota, Columbia, 2003; ISBN 9789583342981.

32. Ferreira, G. Vigas de Concreto Armadas com Taliscas de Bamboo Dendrocalamus Giganteus. Ph.D. Thesis, UNICAMP State University of Campinas, Campinas, Brazil, 2007. [CrossRef]

33. Lewin, M.; Pearce, E.M. Fiber chemistry. In *Handbook of Fiber Science and Technology*; Marcel Dekker Inc.: New York, NY, USA, 1985.

34. Sahu, P.; Gupta, M.K. Sisal (Agave sisalana) fibre and its polymer-based composites: A review on current developments. *J. Reinf. Plast. Compos.* **2017**, *36*, 1759–1780. [CrossRef]

35. John, M.J.; Anandjiwala, R.D. Recent developments in chemical modification and characterization of natural fibre-reinforced composites. *Polym. Compos.* **2008**, *29*, 187–207. [CrossRef]

36. Sahu, P.; Gupta, M.K. A review on the properties of natural fibres and its bio-composites: Effect of alkali treatment. *J. Mater. Des. Appl.* **2020**, *234*, 198–217. [CrossRef]

37. Futami, E.; Shafigh, P.; Katman, H.Y.B.; Ibrahim, Z. Recent Progress in the Application of Coconut and Palm Oil Fibres in Cement-Based Materials. *Sustainability* **2021**, *13*, 2865. [CrossRef]

38. Janssen, J.J.A. *Mechanical Properties of Bamboo*; Springer: Berlin, Germany, 1991. [CrossRef]

39. Yeasmin, L.; Ali, M.N.; Gantailt, S.; Chakraborty, S. Bamboo: An overview on its genetic diversity and characterization. *3 Biotech* **2015**, *5*, 1–11. [CrossRef]

40. Breckle, S.-W. *Walter's Vegetation of the Earth—The Ecological Systems of the Geo-Biosphere*; Springer Publishing: Berlin, Germany, 2002; ISBN 978-3-540-43315-6.

41. Ali, M.; Liu, A.; Sou, H.; Chouw, N. Mechanical and dynamic properties of coconut fibre reinforced concrete. *Constr. Build. Mater.* **2012**, *30*, 814–825. [CrossRef]

42. German Committee for Structural Concrete. *Commentary on the DAfStb Guideline "Steel Fiber Reinforced Concrete" (DAfStb-Issue 614)*; Beuth Publishing: Berlin, Germany, 2015; ISBN 978-3-410-65279-3.

43. Pereira, M.V.; Fujiyama, R.; Darwish, F.; Alves, G.T. On the Strengthening of Cement Mortar by Natural Fibers. *Mater. Res.* **2015**, *18*, 177–183. [CrossRef]

44. Ramli, M.; Dawood, E.T. Effects of palm fiber on the mechanical properties of lightweight concrete crushed brick. *Am. J. Eng. Appl. Sci.* **2010**, *3*, 489–493. [CrossRef]

45. Hwang, C.-L.; Tran, V.-A.; Hong, J.-W.; Hsieh, Y.-C. Effects of short coconut fiber on the mechanical properties, plastic cracking behavior, and impact resistance of cementitious composites. *Constr. Build. Mater.* **2016**, *127*, 984–992. [CrossRef]

46. Baruah, P.; Talukdar, S. A comparative study of compressive, flexural, tensile and shear strength of concrete with fibres of different origins. *Indian Concr. J.* **2007**, *81*, 17–24.

47. Filho, R.D.T.; Ghavami, K.; Sanjuán, M.A.; England, G. Free, restrained and drying shrinkage of cement mortar composites reinforced with vegetable fibres. *Cem. Concr. Compos.* **2005**, *27*, 537–546. [CrossRef]

48. Silva, D.A.; Mobasher, B.; Soranakom, C.; Filho, R.D.T. Effect of fiber shape and morphology on interfacial bond and cracking behaviors of sisal fiber cement based composites. *Cem. Concr. Compos.* **2011**, *33*, 814–823. [CrossRef]

49. Ray, D.; Sarkar, B.K.; Rana, A.K. Fracture behavior of vinylester resin matrix composites reinforced with alkali-treated jute fibers. *J. Appl. Polym. Sci.* **2002**, *85*, 2588–2593. [CrossRef]

50. Widnyana, A.; Rian, I.G.; Surata, I.W.; Nindhia, T.G.T. Tensile Properties of coconut Coir single fiber with alkali treatment and reinforcement effect on unsaturated polyester polymer. *Mater. Today Proc.* **2020**, *22*, 300–305. [CrossRef]

51. Momoh, E.O.; Osofero, A.I.; Menshykov, O. Bond Behaviour of Treated Natural Fibre in Concrete. *Nano Hybrids Compos.* **2022**, *34*, 37–44. [CrossRef]

52. *EN 14651 Test Method for Metallic Fibre Concrete—Measuringthe Flexural Tensile Strength (Limit or Proportionality (LOP), Residual)*; European Committee for Standardization (CEN): Brussels, Belgium, 2005; ISBN 978-0-580-61052-3.

53. Ozerkan, N.G.; Ahsan, B.; Mansour, S.; Iyengar, S.R. Mechanical performance and durability of treated palm fiber reinforced mortars. *Int. J. Sustain. Built Environ.* **2013**, *2*, 131–142. [CrossRef]

54. Zhou, X.; Saini, H.; Kastiukas, G. Engineering Properties of Treated Natural Hemp Fiber-Reinforced Concrete. *Front. Built Environ.* **2017**, *3*, 33–42. [CrossRef]

55. Thomas, B.C.; Jose, Y.S. Impact of sisal fiber reinforced concrete and its performance analysis: A review. *Evol. Intell.* **2019**, *15*, 865–875. [CrossRef]

56. John, V.M.; Cincotto, M.A.; Sjostrom, C.; Agopyan, V.; Oliveir, C.T.A. Durability of slag mortar reinforced with coconut fibre. *Cem. Concr. Compos.* **2005**, *27*, 565–574. [CrossRef]

57. Khan, M.; Rehman, A.; Ali, M. Efficiency of silica-fume content in plain and natural fiber reinforced concrete for concrete road. *Constr. Build. Mater.* **2020**, *224*, 118382. [CrossRef]

58. Ahmad, W.; Farooq, S.H.; Usman, M.; Khan, M.; Ahmad, M.; Aslam, F.; Yousef, R.A.; Abduljabbar, H.A.; Sufian, M. Effect of Coconut Fiber Length and Content on Properties of High Strength Concrete. *Materials* **2020**, *13*, 1075. [CrossRef] [PubMed]

59. Fehling, E.; Schmidt, M.; Walraven, J.; Leutbecher, T.; Fröhlich, S. *Ultra-High Performance Concrete UHPC*; Ernst & Sohn: Berlin, Germany, 2014; ISBN 978-3-433-03087-5.

60. Femandez, J.E. Flax fiber reinforced concrete—A natural fiber biocomposite for sustainable building materials. *High Perform. Struct. Compos.* **2002**, *59*, 15.

61. Athijayamani, A.; Thiruchitrambalam, M.; Natarajana, U.; Pazhanivelc, B. Effect of moisture absorption on the mechanical properties of randomly oriented natural fibers/polyester hybrid composite. *Mater. Sci. Eng. A* **2009**, *517*, 344–353. [CrossRef]

62. Naamandadin, N.A.; Rosdi, M.S.; Mustafa, W.A.; Aman, M.N.S.S. Mechanical behaviour on concrete of coconut coir fiber as additive. *IOP Conf. Ser. Mater. Sci. Eng.* **2020**, *932*, 012098. [CrossRef]

63. Pacheco-Torgal, F.; Jalali, S. Cementitious building materials reinforced with vegetable fibres: A review. *Constr. Build. Mater.* **2011**, *25*, 575–581. [CrossRef]

64. Schmidt, M.; Fehling, E. Ultra-High-Performance Concrete: Research, Development and Application in Europe. *ACI Symp. Publ.* **2005**, *228*, 51–78. [CrossRef]

65. Wiens, U. *Erweiterte Untersuchungen zur Alkalität von Betonen mit hohen Puzzolangehalten*; Fraunhofer IRB Publishing: Stuttgart, Germany, 1999; ISBN 9783816754787.

66. Rao, R.; Stroeven, P.; Hendriks, C.F. Mechanical Properties of Reactive Powder Concrete Beams. *ACI Symp. Publ.* **2005**, *228*, 1237–1252.

67. Ludwig, H.-M.; Thiel, R. Dauerhaftigkeit von UHFB. In *Innovationen im Bauwesen—Ultrahochfester Beton (UHFB)*; Bauwerk-Publishing: Berlin, Germany, 2003.

68. Reinhardt, H.-W.; Jooß, M. Wasserspeicher aus UHFB—Technologie. In *Innovationen im Bauwesen—Ultrahochfester Beton*; Bauwerk-Publishing: Berlin, Germany, 2003.

69. Oettel, V. Torsionstragverhalten von stahlfaserbewehrten Beton-, Stahlbeton- und Spannbetonbalken. Ph.D. Thesis, Technical University of Braunschweig, Braunschweig, Germany, 2016. [CrossRef]

70. Oettel, V.; Rieke, A.; Empelmann, M. Production and testing of thin-walled UHPFRC precast elements. *BFT Int.* **2014**, *80*, 64–74.

71. Bertola, N.; Küpfer, C.; Kälin, E.; Brühwiler, E. Assessment of the Environmental Impacts of Bridge Designs Involving UHPFRC. *Sustainability* **2021**, *13*, 12399. [CrossRef]

72. Habert, G.; Denarié, E.; Šajna, A.; Rossi, P. Lowering the global warming impact of bridge rehabilitations by using Ultra High Performance Fibre Reinforced Concretes. *Cem. Concr. Compos.* **2013**, *38*, 1–11. [CrossRef]

73. Racky, P. Cost-effectiveness and sustainability of UHPC. In Proceedings of the International Symposium on Ultra High Performance Concrete, Kassel, Germany, 13–15 September 2004; pp. 797–805, ISBN 3-89958-086-9.

74. Aitcin, P. Cements of yesterday and today—Concrete of tomorrow, Cem. *Concr. Res.* **2000**, *30*, 1349–1359. [CrossRef]

75. Oettel, V.; Matz, H.; Empelmann, M. Bestimmung der zentrischen Nachrisszugfestigkeit von UHPFRC mithilfe gekerbter 3-Punkt-Biegezugversuche. *Beton-Und Stahlbetonbau* **2019**, *114*, 255–264. [CrossRef]

76. Chan, Y.-W.; Chu, S.-H. Effect of silica fume on steel fiber bond characteristics in reactive powder concrete. *Cem. Concr. Res.* **2004**, *34*, 1167–1172. [CrossRef]

77. Rocky, B.P.; Thompson, A.J. Production of natural bamboo fibers-1: Experimental approaches to different processes and analyses. *J. Text. Inst.* **2018**, *109*, 1381–1391. [CrossRef]

78. Mark, P.; Oettel, V.; Look, K.; Empelmann, M. Neuauflage DAfStb-Richtlinie Stahlfaserbeton. *Beton-Und Stahlbetonbau* **2021**, *116*, 19–25. [CrossRef]

79. Oettel, V.; Lanwer, J.-P.; Empelmann, M. Auszugverhalten von Mikrostahlfasern aus UHPC unter monoton steigender und zyklischer Belastung. *Bauingenieur* **2021**, *96*, 1–10. [CrossRef]

80. Basaldella, M.; Jentsch, M.; Oneschkow, N.; Markert, M.; Lohaus, L. Compressive Fatigue Investigation on High-Strength and Ultra-High-Strength Concrete within the SPP 2020. *Materials* **2022**, *15*, 3793. [CrossRef]

81. Basaldella, M.; Oneschkow, N.; Lohaus, L. Influence of the specimen production and preparation on the compressive strength and the fatigue resistance of HPC and UHPC. *Mater. Struct.* **2021**, *54*, 99. [CrossRef]

82. Liese, W. *The Anatomy of Bambus Colums*; International Network for Bamboo and Rattan: Beijing, China, 1998.

83. *Deutsche Ausschuss für Stahlbeton DAfStb-Richtlinie Stahlfaserbeton: 2021-06*; Beuth-Publishing: Berlin, Germany, 2021.
84. Yoo, D.-Y.; Yoon, Y.-S.; Banthia, N. Flexural response of steel-fiber-reinforced concrete beams: Effects of strength, fiber content, and strain-rate. *Cem. Concr. Compos.* **2015**, *64*, 84–92. [CrossRef]
85. Qian, D.; Yu, R.; Shui, Z.; Sun, Y.; Jiang, C.; Zhou, F.; Ding, M.; Tong, X.; He, Y. A novel development of green ultra-high performance concrete (UHPC) based on appropriate application of recycled cementitious material. *J. Clean. Prod.* **2020**, *261*, 121231. [CrossRef]
86. Shi, Y.; Long, G.; Zeng, X.; Sie, Y.; Wang, H. Green ultra-high performance concrete with very low cement content low cement content. *Constr. Build. Mater.* **2021**, *303*, 124482. [CrossRef]